For 2nd Intern. Conf. on the Strength
of Metals and Alloys, Asilomar, Ca.,
August 30-September 4, 1970

UCRL-20308
Preprint

c.2

METASTABLE AUSTENITES: DECOMPOSITION AND STRENGTH

W. W. Gerberich, G. Thomas, E. R. Parker, and V. F. Zackay

August 1970

RECEIVED
LAWRENCE
RADIATION LABORATORY

SEP 8 1970

LIBRARY AND
DOCUMENTS SECTION

AEC Contract No. W-7405-eng-48

TWO-WEEK LOAN COPY

This is a Library Circulating Copy which may be borrowed for two weeks. For a personal retention copy, call Tech. Info. Division, Ext. 5545

UCRL-20308
c.2

LAWRENCE RADIATION LABORATORY
UNIVERSITY of CALIFORNIA BERKELEY

25

DISCLAIMER

This document was prepared as an account of work sponsored by the United States Government. While this document is believed to contain correct information, neither the United States Government nor any agency thereof, nor the Regents of the University of California, nor any of their employees, makes any warranty, express or implied, or assumes any legal responsibility for the accuracy, completeness, or usefulness of any information, apparatus, product, or process disclosed, or represents that its use would not infringe privately owned rights. Reference herein to any specific commercial product, process, or service by its trade name, trademark, manufacturer, or otherwise, does not necessarily constitute or imply its endorsement, recommendation, or favoring by the United States Government or any agency thereof, or the Regents of the University of California. The views and opinions of authors expressed herein do not necessarily state or reflect those of the United States Government or any agency thereof or the Regents of the University of California.

METASTABLE AUSTENITES: DECOMPOSITION AND STRENGTH

W. W. Gerberich, G. Thomas, E. R. Parker and V. F. Zackay
Inorganic Materials Research Division, Lawrence Radiation Laboratory
Department of Materials Science and Engineering, College of Engineering
University of California, Berkeley, California

Abstract

The stress-strain properties of metastable austenites, including Lüders strain and the strain hardening rate, are quantitatively predicted. This is accomplished by invoking the rule of mixtures, the relationship between the volume of strain-induced martensite, strain and austenite stability, and an empirical description of austenite stability in terms of composition and processing variables.

Introduction

The class of materials under consideration have compositions in the range 0 to 16 Cr, 6 to 35 Ni, 0 to 5 Mn, 0 to 0.5 C+N, 0 to 5 Mo, 0 to 1 V and 0 to 2 Si, which, as had been described earlier, give austenite yield strengths of 50 to 300 ksi after warm working (250-600°C)(1 - 3). Depending upon the test temperature and the stability of the austenite, the amount of martensite strain induced during testing between M_s and M_d can range from a negligible amount to nearly 100 percent. As a result, such mechanical properties as strain-hardening rate and elongation can vary by more than an order of magnitude. Data from 60 different alloy compositions, several of which had as many as 10 different thermal-mechanical histories, are reported. It is important to note that the composition is chosen so that the gamma to martensite transformation occurs and epsilon martensite is avoided as a stable product (4). Discussion is divided into three sections: these treat the development of the mechanical model, a thermal-mechanical-chemical description of austenite stability, and the combination of these to predict mechanical behavior.

Analysis of Mechanical Behavior

Austenite stability, strain and martensite

First, consider a mechanical description of austenite stability. If one measures the volume fraction of martensite, V_α, transformed during a tensile test as a function of conventional strain, ϵ, a unique relationship between V_α and ϵ emerges. For annealed austenitic stainless steels, Angel (5) found a log-autocatalytic type of relationship. In the present class of steels, wherein a certain amount of warm work is usually involved, a somewhat simpler relationship is found as given by (6)

$$V_\alpha = m\epsilon^{\frac{1}{2}} \tag{1}$$

where m is a constant for a given set of test conditions. The value of m would necessarily be zero at the M_d temperature while at temperatures well below M_d, it has been found to be near 3.5. Although this seems to suggest that V_α may be greater than unity, the fact is that failure ensues at an elongation limited to values such that V_α cannot exceed unity. This relationship for tensile data obtained on a 12 Cr-8 Ni-0.5 Mn-3 Mo-0.2 C steel is shown in Fig. 1. As one might anticipate, the rate of martensite formation increases as the test temperature decreases below M_d (145°C for this alloy).

The rule of mixtures

The next assumption is that this two-phase material may be described by the rule of mixtures at any point during extension, viz.,

$$\sigma = \sigma_\alpha V_\alpha + \sigma_\gamma(1 - V_\alpha) \tag{2}$$

where the σ is conventional stress and the γ denotes austenite. Although this may be an oversimplification, it has been shown to be obeyed in the $\gamma - \alpha$ mixtures (3,9). The physical basis for this rule comes from the fact that the $\gamma - \alpha$ mixture is a two-phase mixture of components of different strength levels. The martensite is obviously the stronger since it is substructurally almost fully work-hardened, as has been shown by ausforming studies (7). Thus, the result is a mixture of austenite and hard martensite having semi-coherent interfaces. Mechanically, the system is analogous to fibrous composites.

Structural factors

The parameters involved in producing this mixture relate to austenite stability and martensite nucleation, which implicitly involves plastic strain energy, temperature, composition, deformation mode, etc. The SFE (stacking-fault energy) parameter is of course involved in this since it determines factors such as $\gamma \rightarrow \alpha$ stability through its role in producing the austenite substructure. For example, metallographically, the alloys have the following characteristics: the austenite is severely deformed and in alloys of lower stacking fault energy (with the ratio of Cr, Mn, Mo, V to Ni being about two or greater), it may be mechanically twinned as noted in Fig. 2(b). The strain-induced lath martensite is considerably refined as compared to athermal martensites as shown by Fig. 2(a) and Fig. 2(c). Thus, the deformation characteristics of the austenite determines to some degree the structure and strength of the martensite. In a similar manner, many physical parameters may control the nucleation rate of the strain-induced martensite. It is suggested, however, that the transformation coefficient, m, combines these into a parameter which allows a simple phenomenological treatment of the model.

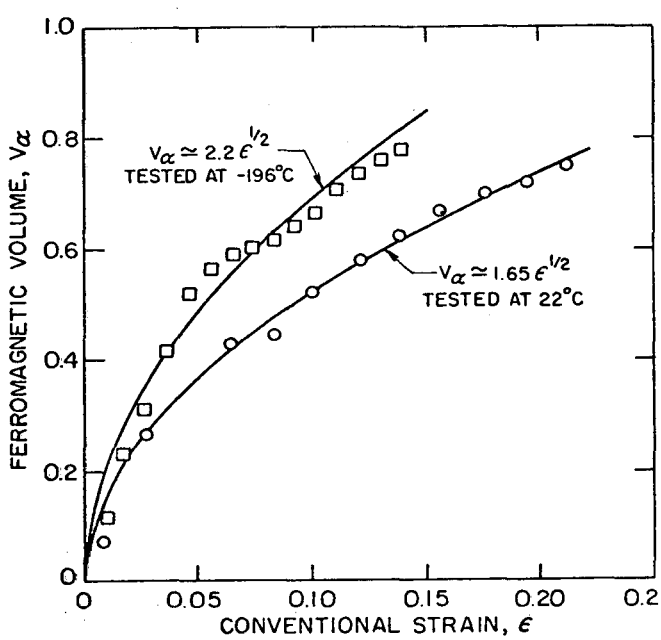

Fig. 1

Relationship between strain and volume fraction of strain-induced martensite for a 12Cr-8Ni-0.5Mn-3Mo-0.2C steel at two different test temperatures.

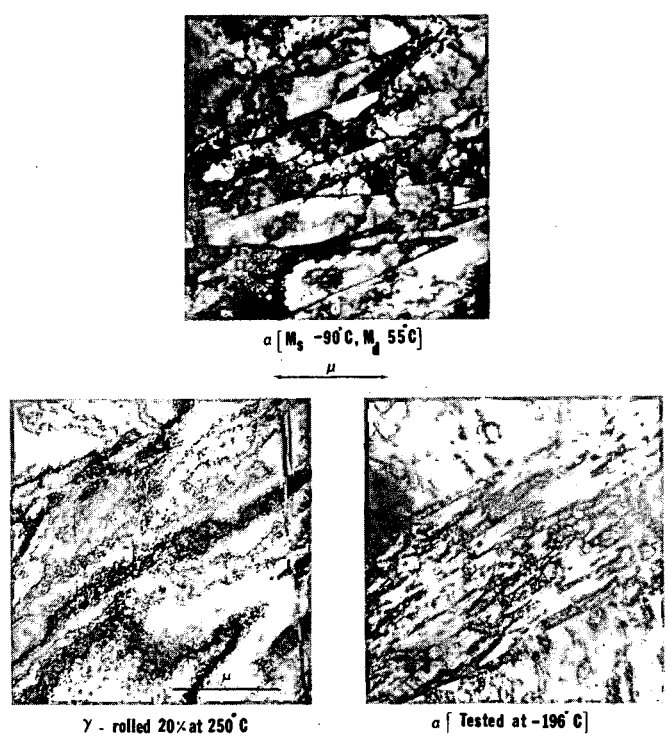

Fig. 2

Transmission electron micrographs of a 9Cr-8Ni-2.4Mn-1.9Si-0.95V-0.08N-0.3C steel: (a) relatively coarse laths in athermal martensite; (b) fine mechanical twins in austenite produced during thermal-mechanical treatment; (c) strain-induced martensite from material shown in (b) results in a fine lath structure. (Courtesy of M. Raghavan)

The Lüders strain

Assume that the strain-hardening required in the Lüders band is governed by the macroscopic stress concentration at the elastic-plastic boundary (8). First, consider that the austenite work hardens to 1.155 times the flow stress. Secondly, consider that the transformation itself contributes to the Lüders strain. The dilatation contribution is directly proportional to the volume fraction of the martensite, while the shear contribution is proportional to the amount of martensite which is aligned with, for example, the macroscopic shear plane. These considerations lead to

$$\varepsilon_L = \frac{0.155\sigma_\gamma e^{\varepsilon_L}}{d\sigma_T/d\varepsilon} + \varepsilon_L^{\frac{1}{2}}\left[\frac{\varepsilon_{IS}}{\sqrt{3}} + m\varepsilon_D\right] \tag{3}$$

where the ε are true strains, the subscripts denote Lüders, invariant shear and dilatational strains and the σ_γ is the conventional flow stress of austenite. The first term on the right hand side of equation (3) represents the austenite contribution while the second term represents the transformation contribution. Taking the linear contribution of the dilatation to be about 0.01 and the shear to be about 0.20, it is possible to calculate the Lüders strain, knowing m and the strain-hardening rate.

The strain hardening rate

Combining equations (1) and (2) gives

$$\sigma = (\sigma_\alpha - \sigma_\gamma)m\epsilon^{\frac{1}{2}} + \sigma_\gamma \tag{4}$$

In terms of true stress, σ_T, and true strain, ε, equation (4) becomes

$$\sigma_T = [\sigma_\alpha - \sigma_\gamma][m(e^\varepsilon - 1)^{\frac{1}{2}}]e^\varepsilon + \sigma_\gamma e^\varepsilon \tag{5}$$

Differentiating and assuming that $\partial\sigma_\alpha/\partial\varepsilon$ and $\partial\sigma_\gamma/\partial\varepsilon$ are negligible compared to the two-phase contribution leads to

$$d\sigma_T/d\varepsilon = \sigma_\gamma e^\varepsilon + me^\varepsilon\,[\sigma_\alpha - \sigma_\gamma][\tfrac{1}{2}e^\varepsilon(e^\varepsilon - 1)^{-\frac{1}{2}} + (e^\varepsilon - 1)^{\frac{1}{2}}] \tag{6}$$

At this point, it is only necessary to describe m, σ_α and σ_γ for evaluation of the strain-hardening rate and Lüders strain from equations (2) and (6). Empirical relationships for both σ_α and σ_γ have been determined from existing data (9) to be

$$\sigma_\gamma \simeq 25 \text{ ksi} + [145 \text{ ksi}/\%C][\text{wt.}\%C][1 + 1.2(\text{P.D.})^2] + 100 \text{ ksi } [\text{P.D.}]^{\frac{1}{2}} \tag{7a}$$

$$\sigma_\alpha \simeq 150 \text{ ksi} + [90 \text{ ksi}/(\%C)^{\frac{1}{2}}][\text{wt.}\%C]^{\frac{1}{2}}[1 + \text{P.D.}] + 50 \text{ ksi } [\text{P.D.}]^{\frac{1}{2}} \tag{7b}$$

where P.D. is the prior deformation amount of austenite in strain units. It is seen that the parabolic work hardening term is more significant in the strength of austenite than in the martensite while the reverse is true with respect to carbon content. As an example of how austenite stability affects the mechanical properties, a large amount of test data for the Lüders strain as a function of m is given in Fig. 3. Also shown are the theoretical curves calculated from equations 3 and 6 for the extremes of $\sigma_\gamma[\sigma_\gamma + (\sigma_\alpha - \sigma_\gamma)]^{-1}$.

Total elongation

Failure is initiated either because of martensite content or because of the lack of strain hardening due to insufficient martensite production in the necked region. These will be denoted as transformation and necking criteria. It was generally observed that those materials obeying a transformation criterion had between 70 and 100 percent martensite at the time of fracture. Using this fact in conjunction with equation (1) leads to the elongation in conventional strain to be given by

$$\epsilon = 1/m^2 \quad \text{for} \quad V_\alpha = 1; \qquad \epsilon = 1/2m^2 \quad \text{for} \quad V_\alpha = 0.7 \tag{8}$$

When the rate of strain-induced martensite is very low, the necking criterion is obeyed as given by $d\sigma_T/d\varepsilon = \sigma_T$. The values of σ_T occurring in the Lüders band is dependent

upon the amount of strain-induced martensite. During the Lüders band formation, if the region in the band contained much less than 40 percent martensite, necking would ensue rather than propagation of the Lüders front. Using 40 percent for V_α in equation (2), describing the true stresses in terms of true strains and then equating this to equation (6), leads to

$$m = 0.8[e^{\varepsilon}(e^{\varepsilon} - 1)^{-\frac{1}{2}} + 2(e^{\varepsilon} - 1)^{\frac{1}{2}}]^{-1} \tag{9}$$

In Fig. 4, it is seen that these criteria describe the elongations observed for tests covering a wide range of alloy contents and test conditions.

Measure of Austenite Stability

The purpose here is to be able to describe the transformation coefficient, m, in terms of M_d; it is first appropriate to define several parameters. M_d is the temperature for the initiation of the strain-induced transformation as normally defined. However, in engineering materials, this temperature is difficult to observe. A somewhat more easily defined parameter from an experimental viewpoint (5) is M^*_{d30} which is the temperature at which a true strain of 30 percent produces 50 percent martensite in an annealed material. It is also convenient to define M_{d30} which is the same type of parameter except that it applies to a material with a thermal-mechanical history. The reason the last two must be differentiated is that prior deformation in the range of 250-600°C precipitates alloy carbides and therefore partially depletes the matrix of carbon and carbide forming elements. From uniaxial tensile data, it was observed that in all cases m increased the further the test temperature was below M_d but that the rate of increase, dm/dT, decreased. A plot of m versus T for five different alloy compositions suggested that the shape of the curve was independent of alloy composition and only dependent upon the test temperature and M_d as given by

$$m \simeq (M_d/160)[(M_d - T)/M_d]^{160/M_d} \tag{10}$$

where the temperatures are in degrees Kelvin. From the same plot, M_{d30} could be interpolated since 50 percent martensite at a true strain of 0.30 is represented by m = 0.85. Furthermore, an intersection of these curves with the abscissa at m equals zero gave a good estimate of the M_d temperature. It was then found that the relationships between M_d, M_{d30} and M^*_{d30} could be simply expressed as

$$M_d \simeq 145°K + 0.725\ (M_{d30}); \qquad M_{d30} \simeq M^*_{d30}\ [1 + C(T_{P.D.})(P.D.) \tag{11}$$

with the limitation that $M_d < 500°K$. Here, C is a constant of 0.00088/°C/unit strain and $T_{P.D.}$ is the temperature of prior deformation which is restricted to temperatures between 100 and 600°C. It is seen that various relationships between m, M_{d30} and M_d can be generated through equations (10) and (11). In fact, it is possible to back calculate M_{d30} given the thermal-mechanical history and the values of m from one tensile test where the ferromagnetic volume was measured. This was done for 35 different alloy compositions from which it was possible to determine the effect of alloy constituents on M^*_{d30}. An example is shown in Fig. 5 where the effect of nickel content on M_{d30} is seen to be about -18.2°C/wt.%Ni. For all alloy constituents, a multiple regression analysis was found to give

$$M^*_{d30}(°K) = 881-490[C+N] - 18.2[Ni] - 20[Cr] - 20[Mo] - 40.8[Mn] \tag{12}$$

where the elements in brackets represent amounts in weight percent. Verification that equations (10-12) represent a reasonable estimate of the transformation coefficient was obtained by comparing the measured value of m to the calculated curves as a function of test temperature and prior deformation amount. This was done for an alloy containing all of the alloying elements given in equation (12). The M^*_{d30} temperature was calculated from equation (12) and then M_d was determined for each thermal-mechanical treatment from equation (11). For each test temperature, it was then possible to calculate m from

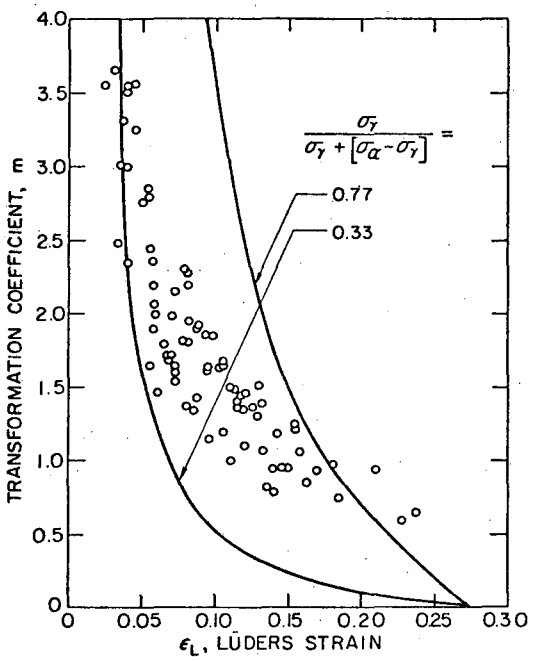

FIG. 3

Effect of transformation coefficient on Lüders strain.

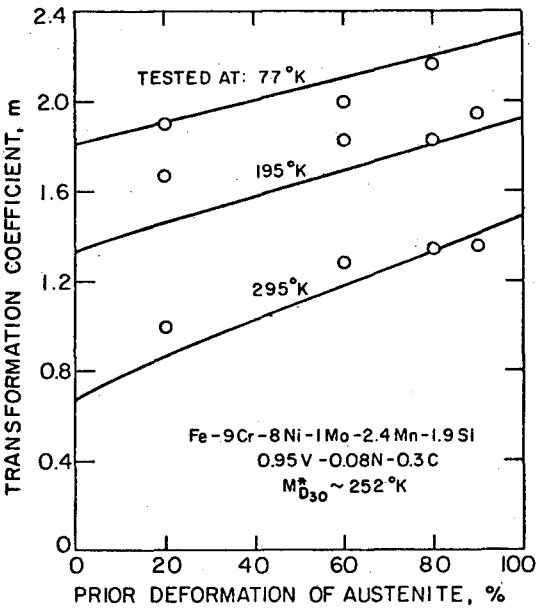

FIG. 6

Comparison of calculated and observed values of the transformation coefficient as a function of test temperature and thermal-mechanical treatment.

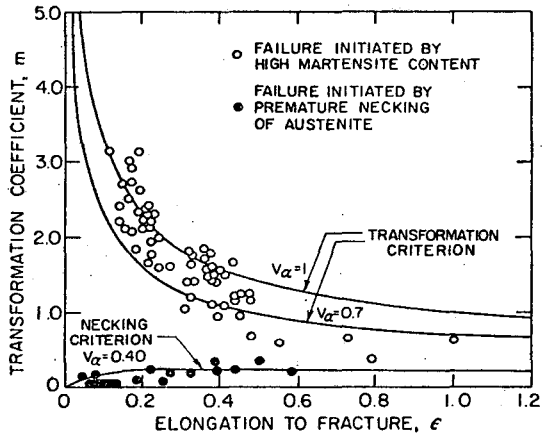

FIG. 4

Effect of transformation coefficient on elongation.

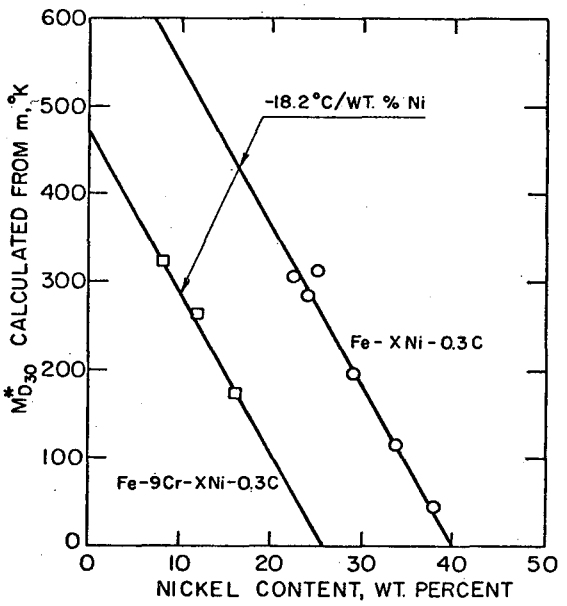

FIG. 5

Relationship between nickel content and austenite stability.

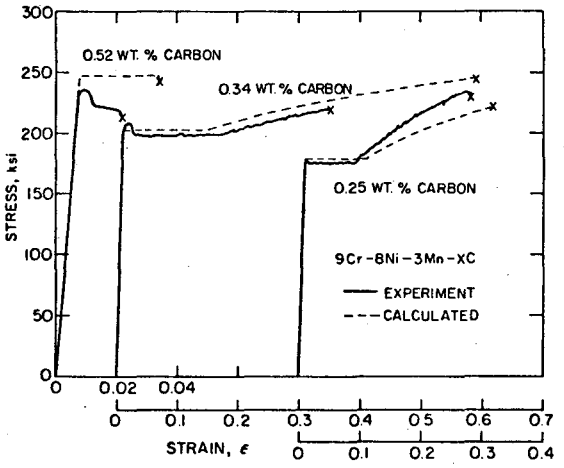

FIG. 7

Prediction of stress-strain behavior for three alloys of different chemical stability.

equation (10). In Fig. 6, it is seen that the calculated curves agree reasonably well with the experimental data.

Prediction of Mechanical Behavior

It is now possible to predict the mechanical properties of these metastable austenites given their prior thermal-mechanical history and composition. The procedure is to determine m from equations (10) - (12) and then use this in equations (3) - (9). For example, it is shown that the stress-strain curves for a series of 9Cr-8Ni-3Mn-XC alloys could be predicted. First, the m values were calculated from the composition and the thermal-mechanical history of 80 percent deformation at 450°C. Then, the austenite flow stress was determined from equation (7a). Calculation of the Lüders strain from equation (2) followed and this was added to the elastic strain represented by the austenite flow stress. At this point, conventional strain-hardening rates were calculated and incremental stresses were added at strain increments of 0.03. Subsequent integration between strain limits showed this procedure to be accurate within one percent. This procedure was followed until the total elongation as governed by either equation (8) or (9) was reached. As seen in Fig. 7, the calculated and experimental curves are in reasonable agreement. The low elongation of the 0.52 wt.%C alloy was due to lack of martensite production and necking was predicted. The only serious discrepancy is in the total elongation of the 0.34 wt.%C alloy. This may be attributed to a premature brittle fracture since no necking was observed and since the final strength of the material should have been greater than the 0.25 wt.%C alloy but was not. In all other respects such as Lüders elongation and strain-hardening rate, the agreement is good.

Acknowledgements

We would especially like to thank M. Raghavan, D. Fahr, J. Dunning, C. Dokko, G. Chanani and D. Bhandarkar for permission to use previously unpublished data. The authors express their appreciation to the United States Atomic Energy Commission for support of this work.

References

1. V. F. Zackay, E. R. Parker, D. Fahr and R. Busch, Trans. ASM, 60, 252 (1967).

2. J. A. Hall, V. F. Zackay and E. R. Parker, Trans. ASM, 62, 965 (1969).

3. P. L. Manganon, Jr. and G. Thomas, Met. Trans. 1, 1577; ibid, 1589 (1970)

4. H. Schumann and von Firchs, Arch. Eisenhuettenw, 40, 561 (1969).

5. T. Angel, J. Iron Steel Inst., 165 (May, 1954).

6. W. W. Gerberich, P. L. Hemmings, V. F. Zackay and E. R. Parker, Fracture 1969, ed. by P. L. Pratt, Chapman and Hall Ltd., London, 288 (1969).

7. G. Thomas, D. Schmatz and W. Gerberich, High-Strength Materials, ed. by V. F. Zackay, J. Wiley and Sons, New York, 251 (1964).

8. G. T. Van Rooyen, Mater. Sci. Eng., 3, 105 (1968/69).

9. W. W. Gerberich, V. F. Zackay and E. R. Parker (in preparation).

LEGAL NOTICE

This report was prepared as an account of Government sponsored work. Neither the United States, nor the Commission, nor any person acting on behalf of the Commission:

A. Makes any warranty or representation, expressed or implied, with respect to the accuracy, completeness, or usefulness of the information contained in this report, or that the use of any information, apparatus, method, or process disclosed in this report may not infringe privately owned rights; or

B. Assumes any liabilities with respect to the use of, or for damages resulting from the use of any information, apparatus, method, or process disclosed in this report.

As used in the above, "person acting on behalf of the Commission" includes any employee or contractor of the Commission, or employee of such contractor, to the extent that such employee or contractor of the Commission, or employee of such contractor prepares, disseminates, or provides access to, any information pursuant to his employment or contract with the Commission, or his employment with such contractor.

TECHNICAL INFORMATION DIVISION
LAWRENCE RADIATION LABORATORY
UNIVERSITY OF CALIFORNIA
BERKELEY, CALIFORNIA 94720